2014 14th IEEE-RAS International Conference on
Humanoid Robots (Humanoids)
November 18-20, 2014. Madrid, Spain

Towards the Development of a Minimal Anthropomorphic Robot Hand

Donald Dalli, *Student Member, IEEE* and Michael A. Saliba, *Senior Member, IEEE*

***Abstract*— Many robot hands in the literature try to achieve full kinematic anthropomorphism, and as such are often very complex and difficult/expensive to produce. This paper follows recent work that predicts that high dexterity can also be achieved through a minimal (reduced) anthropomorphic design. New experimental and simulation results that optimize grasping performance for a minimal hand are presented. A first prototype of the hand, incorporating the optimized kinematics as well as innovative endoskeletal mechanical and actuation architectures, has been designed. The robot hand prototype has been fabricated using fused deposition modelling technology, and is evaluated with respect to its grasping performance.**

I. Introduction

The dexterous capabilities of the human hand are highly attributed to the densely packed mechanisms found inside it, resulting in a system of 21 degrees of freedom (DOFs). This has often inspired researchers to develop anthropomorphic robotic hands that replicate the functions of the human counterpart. However, this replication in the form of a robotic device has often been one of the major engineering challenges, due to the difficulty encountered in incorporating several coordinated mechanisms under stringent space and weight limitations.

Such robotic devices are intended to manipulate objects that were originally designed for humans. Despite careful designing, numerous robotic hands often either lack considerable dexterous capabilities, or employ complex structures and subcomponents therefore leading to high manufacturing costs. Hence, the compromise between complexity of the design and dexterity of the artificial hand is key to an effective robotic hand design.

To overcome this design challenge, several authors presented innovative approaches to enhance the dexterity of robotic hands. Okada [1] developed a highly compact robotic hand aimed for industry, having two fingers and a thumb. Tendon cables passing through the finger tubes are driven by d.c. motors. Fukaya *et al.* [2] constructed an artificial hand with 20 DOFs, consisting of a series of links that can be driven by a single actuator, hence facilitating the system control. Lotti *et al.* [3] developed a robot hand (UBH3), with cables routed inside the endoskeletal structure. As the actuators pull the cables, the skeletal elements revolve about steel spiral coils that act as the joints of the robotic hand.

However, the robot hand designs presented in literature are mostly based on the respective authors' own design approaches and intuitions. This is mainly due to the lack of availability of supportive design guidelines in this field. Although in most cases the end objectives are the same, the foundations of these robot hands differ significantly from one design to another.

In a recent study [4], a novel approach was taken to provide a set of supportive design guidelines based on quantitative results. A series of constrained human manual dexterity tests were conducted to identify the contribution of each joint in the fingers. It was determined that the index finger, the middle finger and the thumb were sufficient to carry out a range of dexterous tasks. By applying this knowledge to the field of robotics, a minimal robot hand can be hypothesized. This will in theory be capable of attaining levels of dexterity comparable to that of the human hand, while employing minimum complexity.

In this work, a first prototype of a minimal robotic hand based on the configuration proposed in [4] has been developed. This prototype focuses on attaining the *structural*, *kinematic*, and *actuator transmission* systems for the artificial hand, and does not as yet address the minimal *force*, *sensory* and *control system* requirements. The dexterity of the robot hand was assessed on its ability to perform a series of power and precision grasps outlined by Cutkosky in [5]. Moreover, an innovative mechanical architecture has been adopted to reduce the number of parts and complexity involved, and hence ease the manufacturing process.

Due to its potential high dexterity, its inherent simplicity (with association to low cost and high robustness/reliability), and its basic anthropomorphism, an artificial hand of this nature offers significant potential for applications in humanoid robots and in prosthetics.

II. Dexterity

A. Hand Grasping

The human hand is capable of grasping and manipulating objects of different geometries in various ways. These capabilities reflect the dexterity of the hand. The study and identification of the grasps that can be performed by the human hand enable the foundations for the design of the robot hand [5]. However, the identification and classification of all grasps has often been a challenging task, since grasps, in general, involve the combination of more than one finger [6].

Cutkosky [5] stated that the type of grasp performed by the hand is principally based on the task that the individual seeks to accomplish with the object. His grasping taxonomy consists of a total of sixteen principal grasps, listed in Table I. The notation in Table I will be used to refer to the different grasps throughout this text.

B. Robot Hand Dexterity

One of the main factors that have impeded the entry of robotic hands into human environments is their limited versatility and dexterity. This problem is often encountered

D. Dalli and M. A. Saliba are with the Robotics and Industrial Automation Laboratory (RIAL) of the Department of Industrial and Manufacturing Engineering of the University of Malta, Msida, Malta MSD 2080 (phone: +356-9945-8660; fax: +356-2134-3577; e-mail: michael.saliba@um.edu.mt).

TABLE I. ALL GRASPS AS OUTLINED BY CUTKOSKY [2]

Power Grasps		Precision Grasps	
G1	Large Diameter	**G10**	Tripod
G2	Small Diameter	**G11**	Sphere
G3	Medium Wrap	**G12**	Disk
G4	Adducted Thumb	**G13**	Thumb & Index Finger
G5	Light Tool	**G14**	Thumb & 2 Fingers
G6	Disk	**G15**	Thumb & 3 Fingers
G7	Sphere	**G16**	Thumb & 4 Fingers
G8	Platform		
G9	Lateral Pinch		

in robotic devices that involve classical mechanical designs, which usually consist of pulleys, gears and rigid links [7-10]. Structural compliance was regarded as a defect of the system, hence robot hands were designed to be stiff and rigid. Most often, such robot hand designs employed an *exoskeleton structure*, whereby the actuation of the system was built inside the robot hand to maintain accuracy. As a result, such robot hands are often rather bulky, heavy and require high manufacturing costs.

In more recent years, researchers have recognised that by implementing non-conventional mechanisms and effective control of the compliance of the system, the performance of a robot hand could be enhanced [11]. Compliant mechanisms are able to absorb the energy during impact without being damaged, making them robust in "unstructured" human environments. Usually, but not always, such designs are associated with an *endoskeleton structure*, whereby the actuation system is remotely located away from the hand, hence mimicking the anatomical structure of the human hand. Such structure eases the space constraints in the robot hand design, hence resembling better the human hand.

C. Minimal Design Guidelines

Saliba *et al*. [4] in their work extracted the following kinematic attributes for a minimal artificial anthropomorphic dexterous robot hand:

- The inclusion of an index finger, a middle finger and a thumb, actuated through base joints (corresponding to the human metacarpophalangeal (MCP) joints) and second flexion joints (corresponding to the human proximal interphalangeal (PIP) joints of the fingers and the human distal interphalangeal (DIP) joint of the thumb).
- The inclusion of DIP (i.e. third flexion) joints on the fingers, coupled to the PIP joints, as in the human counterpart [12], with an angular ratio of

$$\theta_{\mathrm{DIP}} = {}^{2}/_{3}\, \theta_{\mathrm{PIP}} \qquad (1)$$

- Maximum flexion angles of the PIP and MCP joints of 110° and 90°, respectively, based on [12].
- The inclusion of one abduction/adduction joint between the two fingers, with a range of angular motion similar to that of the human fingers, i.e. of about 30° [12].
- The inclusion of two additional degrees of freedom to the thumb, equivalent to the rotation and abduction / adduction motions of the human trapezoid-metacarpal (TM) joint.

The paper postulated that an artificial hand with only the above kinematic attributes would be capable of attaining a dexterity (as would be quantified through standard grasping / manipulation tests) of about 84% of the full unfettered human hand, as long as all of the other attributes of the artificial hand (force, sensory and control capabilities, as well as visual feedback and an information database) were equivalent to those of a human.

With regard to the thumb, the paper suggested that further investigation may be required to complement an earlier study conducted by the German Aerospace Center (DLR) [13]. In their work, the DLR included the following suggestions for an effective mechanical thumb in a robot hand:

- The thumb should at least have 3 DOFs for proper manipulation.
- The joint axis of the MCP and DIP are slightly inclined to improve the orientation of the thumb during contact.
- The ratio of the length of the bones should follow an anthropomorphic scale.

All of the above design guidelines were used as the basis for the preliminary experimental and simulation tests conducted in this work, described in Sections III and IV below.

III. PRELIMINARY EXPERIMENTAL WORK

Since the present work focuses on grasping rather than manipulation dexterity, the proposed reduced hand configuration was initially tested out on a human hand by performing the series of grasps listed in Table I, while constraining the ring and little fingers using a set of bandages.

It was immediately clear that the grasps G15 and G16 could not be performed due to the suppression of the ring and little fingers. Hence, this already induces a penalty on the overall grasping performance of the robot hand. The constrained hand was tested for the fourteen remaining grasps. Any adjustments that had to be made to the posture of the constrained hand were noted. This was central to the development of the hand simulation (Section IV), as it dictated the ultimate kinematic structure of the robot hand. Some of the results of these tests are shown in Fig. 1.

In general, the remaining fourteen grasps could be performed using the constrained human hand configuration. The precision grasps felt more natural to perform than the power grasps. Nonetheless, some adjustments to the grasping postures had to be performed. In fact, during the *large diameter* grasp (G1), it was noted that the two fingers were too close to each other, which caused stability issues in holding the object securely. Hence, greater force had to be exerted by the fingers to hold the object in place. With regard to the respective power and precision grasps of the *disk* in G6 and G12, increased effort had to be exerted during the abduction of the two fingers, to compensate for the absence of the ring and little fingers.

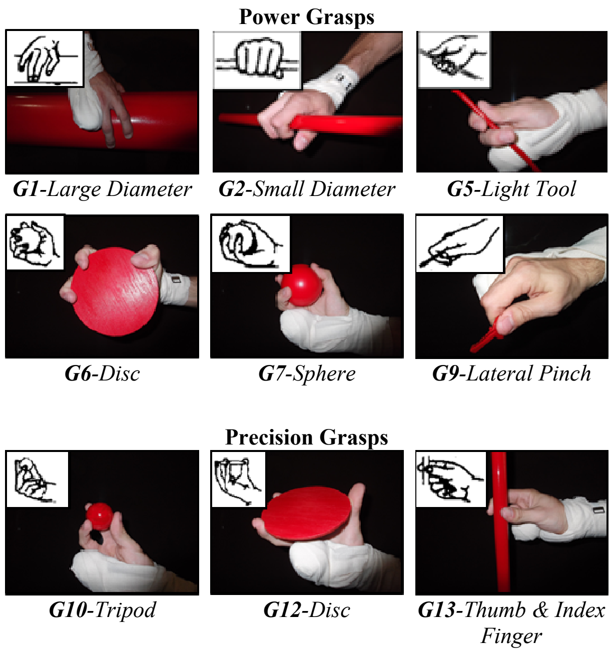

Figure 1. Cutkosky grasps performed by a human using the proposed hand configuration.

IV. Hand Simulation

A simulation of the kinematic hand model was constructed in Autodesk Inventor [14] and enabled the extraction and optimization of quantitative data related to the kinematics of the robot hand. Thus, a dexterous model with the least possible number of independent controllable joints could be systematically developed. The grasping capability of the kinematic model was determined by its ability to perform the fourteen grasps deduced earlier from Section III.

To optimize the kinematic structure of the robot hand, various parameters, such as the lengths of the phalangeal bones and the positioning of the fingers, could be adjusted in the simulation. Moreover, other parameters related to the thumb were included, as shown in Fig. 2. The position of the thumb relative to the hand depends on the *Thumb Position X* (T_{PX}), *Thumb Position Y* (T_{PY}) and *Thumb Position Z* (T_{PZ}). The inclination angle of the DIP and MCP joints of the thumb are described by the *Thumb Distal interphalangeal joint* (T_{DJ}) and *Thumb Metacarpophalangeal joint* (T_{MJ}), suggested in [13]. The *Thumb Natural Twist* (T_{NT}) angle was also varied to optimize the results.

Finally, it was required to attempt to decrease the DOFs of the thumb to three, without significantly compromising the hand dexterity. In order to remove the least effective DOF, two other structural parameters were introduced, namely the *Thumb Orientation X* (T_{OX}) and *Thumb Orientation Z* (T_{OZ}). Hence in the simulation, the orientation of the thumb could be varied along these two axes. The DOFs of the thumb were suppressed systematically, until the least effective DOF was identified. From the conducted simulations, it was observed that the abduction/adduction motion of the thumb could be sacrificed, provided that the thumb orientation angles are adjusted for optimal compensation of this deficiency.

The above mentioned parameters were varied systematically, each time producing a different kinematic model. For each different kinematic model that was created, the fourteen grasps were reproduced by controlling the joints of the model in the simulation. It was observed that the variation of the axes T_{OZ} and T_{OX}, had significant effects on the grasps.

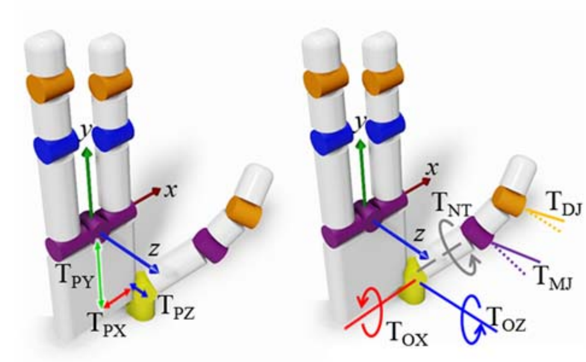

Figure 2. Simulated hand model showing the variable parameters related to the thumb.

The best results were obtained for $T_{OZ} = 30^o$ and $T_{OX} = 15^o$. This configuration resulted in 13 successful grasps, out of the 14 possible grasps, and hence it was selected as the kinematic model for the robot hand. The failed grasp was the *large diameter* grasp (G1), which was also unsuccessful in the other simulation models. This failure was due to the suppression of the abduction/adduction degree of freedom of the thumb, making it very difficult for the whole hand model to open up to grasp large diametrical objects.

The final kinematic model consists of 10 joints with 8 independent DOFs, which include the 3 DOFs of the thumb, 2 DOFs and 2 passive joints in each finger, and 1 DOF for the finger abduction/adduction motion. Some of the grasps performed by the final simulation model are shown in Fig. 3.

From the results obtained, it was observed that the contribution of the DIP coupled joint to fingertip motion was crucial to both power and precision grasps. Also, another important observation was that the phalangeal lengths should be set such that a closed loop can be formed by touching the

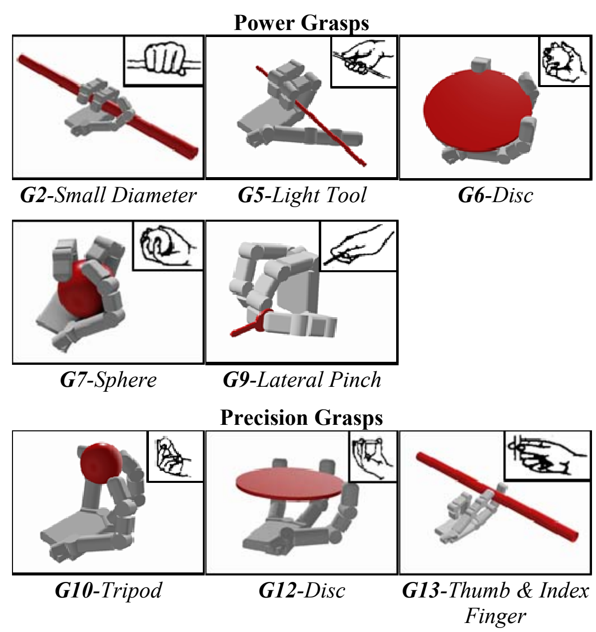

Figure 3. Cutkosky grasps performed using the hand simulation based on the developed kinematic structure

tips of the fingers and thumb. This feature plays an important role during power grasps. The abduction/adduction motion of the fingers was slightly adjusted to compensate for the absence of the ring and little finger. Instead of having the abduction/adduction motion varying from -15^o to $+15^o$, it was adjusted to vary from 0^o to $+30^o$ for improved results. Finally, T_{DJ} and T_{MJ} were both set to 5^o, as it improved the grasping capabilities during thumb opposition.

V. Robot Hand System Design and Fabrication

A. Target Specifications

The aim of this work was to design a minimal human-scale robotic hand that retains a reasonable level of grasping capabilities whilst also retaining anthropomorphic features. The design guidelines listed in Section IIC, together with the results of the above experimental and simulation work enabled the development of the key features for the mechanical design. This first prototype focused on attaining the kinematic capabilities of the equivalent constrained human hand.

The number of parts and the assembly operations of the robotic device had to be limited, to facilitate its production and reduce its cost. Also, the robotic hand had to be independent of the actuators used and of the control system, enabling it to be integrated to diverse systems to manipulate the hand. To overcome these engineering challenges non-conventional techniques were utilized and are presented in the following sections.

B. General Mechanical Framework

Due to the potential reduction in mechanical complexity and the higher degree of anthropomorphism, the design of the new robot hand adopted an endoskeletal structure, composed of modular skeletal elements. The elements were designed for fabrication using fused deposit modelling (FDM) technology. This technology enables compact complex geometries to be produced out of ABS plastic.

Eight remotely located Firgelli Electric Linear Actuators [15], were selected to effect the contraction motion for a more compact design. Transmission was affected via a series of cables, to imitate the tendons found in the human forearm.

C. Joint Mechanism

Alternative solutions, other than the traditional hinge mechanism, were explored during the design process. A novel joint mechanism was developed, with the aim of reducing the mechanical complexity. Fig. 4 shows the final joint mechanism implemented in the robot hand; its working principle is described below.

As in Fig. 4, a tendon cable is first fixed to the distal element of the robot hand to be controlled and then passed through the intermediate element below. As the linear actuator pulls the cable, the distal element rotates due to the curved geometry of the interface between the distal and intermediate elements. This causes the flexion motion of the finger. An elastic strip on the back of the joint is used to store energy while the tendon cable is pulled. As the load on the cable is released, the elastic strip restores its energy and returns the distal element to its neutral position, i.e. extension of the finger takes place. Moreover, this elastic strip improves the compliance of the system. This enables two-directional control of the joint with only one powered actuator.

This mechanism was adopted on all the joints of the robot hand. Minor modifications were made according to the range of angular motion of each joint.

D. Transmission System

A series of routing channels were designed into the skeletal elements of the robotic hand. Fig. 5 shows an example of the channels, which enable the cables to be efficiently routed through the fingers without interfering with each other. The channels also ensure that the cables always pass along the same path, to ensure that their effective lengths do not change during actuation. This enables the cables to remain tensioned throughout the motion cycles. The use of the 3D-printing technology facilitated the fabrication of the complex geometries of these routed channels.

It was ensured that the movement of one joint does not affect the movement of the subsequent joints. To minimize unnecessary coupling, the routed channels were passed as close as possible to the centre of rotation of these joints.

As discussed earlier, the DIP and PIP joints were coupled together with a ratio of 2:3. To obtain this motion, the distances R_{DIP} and R_{PIP} (Fig. 6) were set to this ratio (6 mm and 4 mm, respectively). The associated tendon cables were attached to the same actuator. As the linear actuator retracted, the DIP and PIP joints flexed simultaneously, producing a motion similar to that of the human finger.

E. Final Design of the Robot Hand

The final dimensions of the robotic hand are shown in Fig. 7. Most of the important dimensions were derived from the simulation results. The angular range of abduction/adduction motion of the fingers is indicated by the 30^o angle shown in the figure. The thumb inclinations have also been included, as indicated by the 5^o angles.

F. System Control

A microcontroller (Arduino Mega 2560 [16]) was used to instruct the actuators to the required positions. Custom programs were developed and loaded onto the microcontroller to optimize the performance of the actuators.

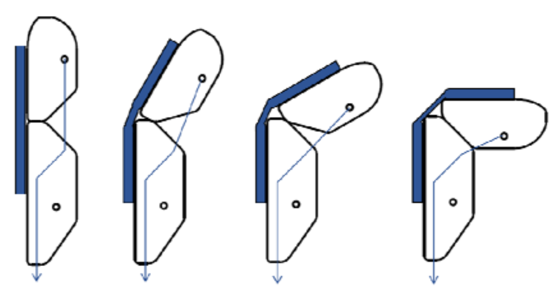

Figure 4. Principle of operation of the developed joint mechanism

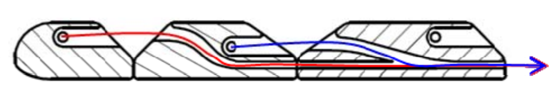

Figure 5. Cross-section of the finger showing the routed channels which allow the cables to pass through the digits.

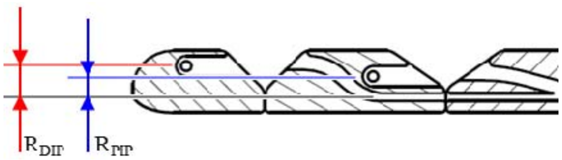

Figure 6. Cross-section of the finger showing the distances between the centre of rotation (contact point) of the joints and the fixing point of the cables.

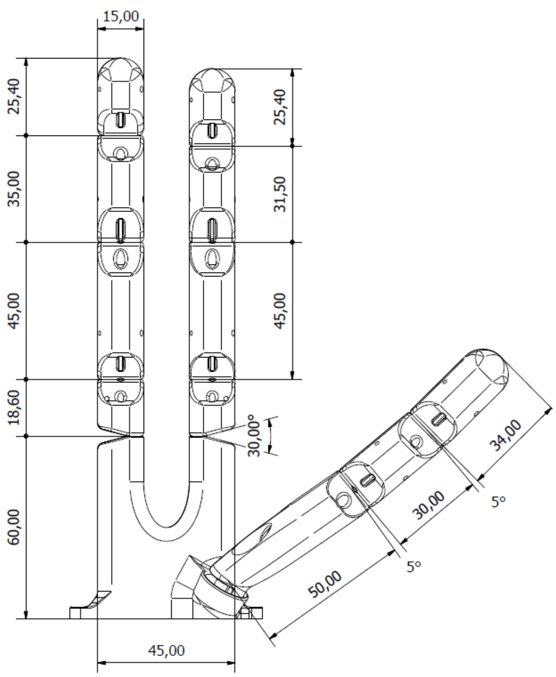

Figure 7. Final dimensions of the robot hand (Dimensions are in mm).

Two alternative input devices were designed to be integrated with the system. The first is a handheld device, containing eight rotary potentiometers (Fig. 8a). The position of each potentiometer is read by the microcontroller and converted to the corresponding actuator position. A glove input device (Fig. 8b) was also developed to facilitate the robot hand operation. This device makes use of a series of flexible bend sensors [17], strategically placed on the glove to effectively read the angular positions of the fingers.

G. Fabrication

The final robot hand was produced using FDM technology with the *Dimension 1200es* fabrication tool [18] available in our laboratory. The whole fabrication process of the plastic parts took less than 12 hours to complete, and required an over-night stay in a water-based solution to remove the excess support material. The actuation system together with the necessary circuitry was enclosed inside a metal case, as shown in Fig. 9.

VI. Evaluation of the Robot Hand

The developed robotic hand was tested for its ability to perform the grasps predicted by the simulation. The robot hand performed well during these tests, as it was capable of performing all of the predicted grasps. This was attributed to the optimized kinematic design, as well as to the compliance of the system that resulted from the new joint mechanism, that enabled the fingers to wrap easily around the objects. Some of the grasping results are shown in Fig. 10. In later tests, a soft glove was put on the robot hand, to improve the gripping surface and increase the contact area during grasping. Some of the improved results are shown in Fig. 11.

The use of FDM resulted in low manufacturing costs, as well as in a low number of parts, since this technology enables geometrical features to be readily 3D printed into the parts. Moreover, the weight of the robot hand on its own is very low, just under 100 g, making it ideal for various robotic applications with limited payloads and for prosthetic devices.

Preliminary quantitative evaluation of the robot hand indicated a non-linearity positional error of ±4% using the handheld input device, and of ±12% using the glove. The latter error can be improved significantly through calibration, however our current effort in this regard is focused on revising and optimizing the overall glove design.

Experimental measurement of the fingertip force capability of the prototype hand demonstrated a maximum of 2.6N and 1.8N by the thumb and the fingers, respectively. This is about an order of magnitude less than that of a healthy human subject (see, for example, [19]).

VII. Conclusion

In this work, a minimal anthropomorphic robot hand was developed, having only two fingers and a thumb, resulting in a system of a total of eight DOFs. Simulation tests were conducted to optimize the kinematic structure with respect to grasping capability. A minimal mechanical architecture was designed, significantly lowering the number of parts required

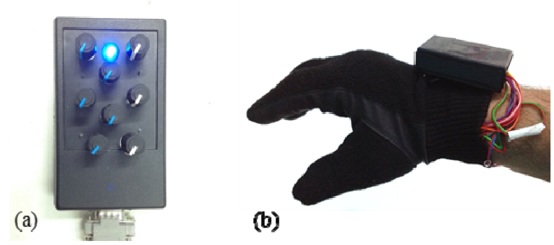

Figure 8. (a) Handheld input device containing eight potentiometers; (b) Glove input device containing eight flexible bend sensors

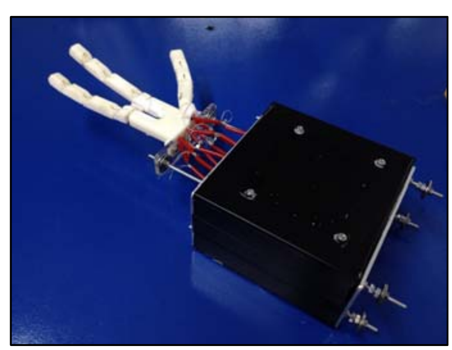

Figure 9. The final robot hand connected to the actuation system.

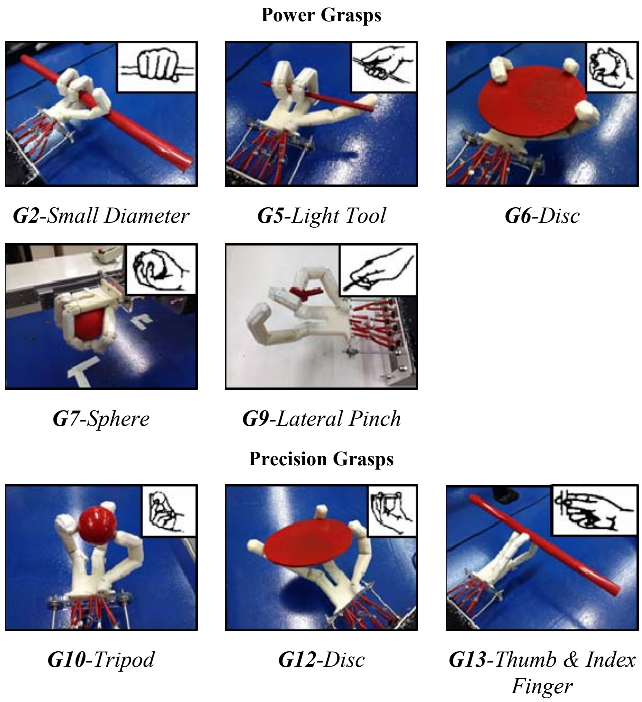

Figure 10. Cutkosky grasps performed using the developed robot hand

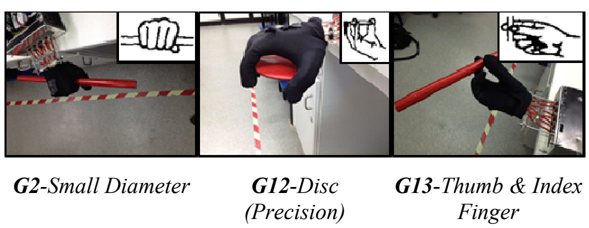

Figure 11. Some grasps performed using the compliant glove

and the overall weight of the system. The modular approach to the design, as well as the fast fabrication method that is utilized, allow for future improvements to the kinematic design to be easily accommodated.

The robot hand has demonstrated a satisfactory level of performance, as it is capable of attaining the grasps predicted by simulation. However, in order for the system to approach the upper limit of dexterity described in [4], it would need to be equipped with better, closed-loop, finger positional control, and further integrated with visual, tactile and high level control systems equivalent, performance-wise, to that of the human. Other factors such as surface compliance and skin texture found in the human hand, must also be considered in the robot hand to improve its dexterity.

The robot hand developed in this work had its design parameters optimized with respect to the grasping dexterity, rather than to the manipulation dexterity. However, this step is crucial to the study, as it lays out the necessary foundations for further developments. Ongoing work aims to extract a comprehensive set of quantitative data on the developed robot hand, as well as to improve the glove input device. Future work is expected to involve the development of a new robot hand prototype with improved force capabilities, as well as with manipulation dexterity, in order to establish improved design guidelines for a minimal anthropomorphic robot hand.

VIII. Acknowledgment

This work was partly funded under University of Malta Research Grant IMERP-03-04.

References

[1] T. Okada, "Object-handling system for manual industry," *IEEE Transactions on Systems, Man and Cybernetics,* vol. 9, *1979,* pp. 79-89.

[2] N. Fukaya, S. Toyama, T. Asfour, and R. Dillmann, "Design of the TUAT/Karlsruhe humanoid hand," in *Proceedings of the IEEE/RSJ International Conference on Intelligent Robots and Systems*, vol.3. 2000, pp. 1754-1759.

[3] F. Lotti, P. Tiezzi, G. Vassura, L. Biagiotti, C. Melchiorri, and G. Palli, "UBH 3: A biologically inpired hand," *IEEE International Conference on Intelligent Manipulation and Grasping, Genoa, Italy,* 2004, pp. 39-45.

[4] M. A. Saliba, A. Chetcuti, and M. J. Farrugia, "Towards the rationalization of anthropomorphic robot hand design: Extracting knowledge from constrained human manual dexterity testing," *International Journal of Humanoid Robotics,* vol. 10, 2013, p. 1350001.

[5] M. R. Cutkosky, "On grasp choice, grasp models, and the design of hands for manufacturing tasks," *IEEE Transactions on Robotics and Automation,* vol. 5, 1989, pp. 269-279.

[6] I. M. Bullock and A. M. Dollar, "Classifying human manipulation behavior," *IEEE International Conference on Rehabilitation Robotics,* 2011, pp. 1-6.

[7] S. C. Jacobsen, E. K. Iversen, D. Knutti, R. Johnson, and K. Biggers, "Design of the Utah/M.I.T. dextrous hand," in *IEEE International Conference on Robotics and Automation.*, 1986, pp. 1520-1532.

[8] C. S. Lovchik and M. A. Diftler, "The Robonaut hand: a dexterous robot hand for space," in *IEEE International Conference on Robotics and Automation, 1999*, vol.2, pp. 907-912.

[9] T. Mouri, H. Kawasaki, K. Yoshikawa, J. Takai, and S. Ito, "Anthropomorphic robot hand: Gifu Hand III," *Proceedings of the Internation Conference on Control, Automation and Systems,* 2002, pp. 1288-1293.

[10] C. Borst, M. Fischer, S. Haidacher, H. Liu, and G. Hirzinger, "DLR hand II: experiments and experience with an anthropomorphic hand," in *IEEE International Conference on Robotics and Automation, 2003,* pp. 702-707.

[11] L. Biagiotti, F. Lotti, C. Melchiorri, and G. Vassura, "Mechatronic design of innovative fingers for anthropomorphic robot hands," *IEEE International Conference on Robotics and Automation, 2003,* pp. 3187 - 3192.

[12] J. Lin, W. Ying, and T. S. Huang, "Modeling the constraints of human hand motion," in *Workshop on Human Motion, 2000*, pp. 121-126.

[13] M. Chalon, M. Grebenstein, T. Wimbock, and G. Hirzinger, "The thumb: guidelines for a robotic design," in *IEEE/RSJ International Conference on Intelligent Robots and Systems* 2010, pp. 5886-5893.

[14] Autodesk. (2014). *Inventor*. Available: http://www.autodesk.com/products/autodesk-inventor-family/overview

[15] Firgelli Technologies Inc., *Miniature Linear Motion Series - L12*.

[16] Arduino. (2014). *Arduino Mega 2560*. Available: http://arduino.cc/en/Main/arduinoBoardMega2560

[17] FlexPoint Sensor Systems Inc., *Bend Sensor Technology Electronic Interface Design Guide*, 1997.

[18] Stratasys. (2014). *Dimension 1200es*. Available: http://www.stratasys.com/3d-printers/design-series/performance/dimension-1200es

[19] C.G. Burgar, F.J. Valero-Cuevas, and V.R. Hentz, "Fine-wire electromyographic recording during force generation: Application to index finger kinesiologic studies", *American Journal of Physical Medicine & Rehabilitation* vol. 76 Iss. 6, 1997, pp. 494-501.